Generative Modeling of Labeled Graphs under Data Scarcity

Sahil Manchanda* **Shubham Gupta*** **Sayan Ranu** **Srikanta Bedathur**

Department of Computer Science and Engineering
Indian Institute of Technology Delhi
{sahil.manchanda,shubham.gupta,sayanranu, srikanta}@cse.iitd.ac.in

Abstract

Deep graph generative modeling has gained enormous attraction in recent years due to its impressive ability to directly learn the underlying hidden graph distribution. Despite their initial success, these techniques, like many of the existing deep generative methods, require a large number of training samples to learn a good model. Unfortunately, a large number of training samples may not always be available in scenarios such as drug discovery for rare diseases. At the same time, recent advances in few-shot learning have opened door to applications where available training data is limited. In this work, we introduce the hitherto unexplored paradigm of *labeled graph generative modeling under data scarcity*. Towards this, we develop GSHOT, a meta-learning based framework for *labeled* graph generative modeling under data scarcity. GSHOT learns to transfer meta-knowledge from similar auxiliary graph datasets. Utilizing these prior experiences, GSHOT quickly adapts to an unseen graph dataset through *self-paced fine-tuning*. Through extensive experiments on datasets from diverse domains having limited training samples, we establish that GSHOT generates graphs of superior fidelity compared to existing baselines.

1 Introduction and Related Work

With recent advances in deep learning, there has been a surge in developing deep graph generative methods that directly learn the underlying hidden distribution of graphs from the data itself [1–10]. These techniques have shown significant improvement over the traditional methods for the graph generation task. Since many real-world graphs such as protein interaction networks [11] and drug molecules [12] are labeled and originate from diverse domains, our focus is on learning *domain-agnostic*, *labeled* graph generative [2, 13] model which jointly models the relationships between a graph structure and its node/edge labels.

A well-known fact about deep generative models is that they are not well suited for applications where training data is scarce [14]. In our study, we observe similar trends for graph deep generative modeling. In Fig. 1a we study the impact of limiting the number of training samples available to GRAPHGEN [2], which is the state-of-the-art method for domain agnostic labeled graph generation. We observe that GRAPHGEN's performance deteriorates significantly[2] when the size of the training dataset is reduced.

The lack of training graphs is often severe in many important settings such as effective drug discovery for rare diseases [15] or speedy drug discovery during pandemics such as COVID-19 [16]. Similar issue appears in physics while developing generative models for computationally expensive *N-body* simulations [17–19].

In this context, we observe that although the availability of graphs exhibiting a specific desired property may be limited, it may be possible to identify graph repositories exhibiting similar properties.

*Equal contribution.

[2]See Sec. 4.1 for detailed understanding of the metrics.

, Generative Modeling of Labeled Graphs under Data Scarcity. *Proceedings of the Second Learning on Graphs Conference (LoG 2023)*, PMLR 198, Virtual Event, November 27–30, 2023.

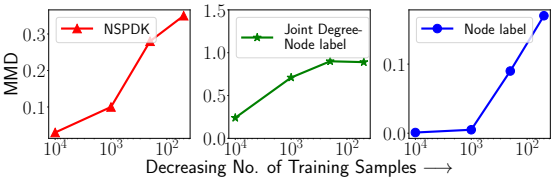

(a) Performance vs Number of training samples

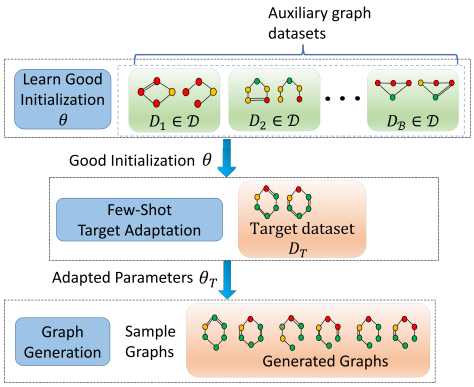

(b) The pipeline of steps in GSHOT.

Figure 1: (a) Increase in Maximum Mean Discrepancy (MMD) scores for different graph metrics when the number of training samples (log scale) are decreased in a chemical compound dataset (Dataset #2 in Table 3) for GRAPHGEN [2]. A higher MMD corresponds to poor fidelity. **(b)** Our proposed architecture.

To elaborate, we may not have access to a large set of molecules exhibiting activity against COVID-19. However, million-scale repositories of chemical compounds are widely available [20], from which the broad characteristics of chemical compounds such as valency rules, correlated functional groups, etc. may be learned. Hence, potentially, the learning task from the smaller COVID-19 repository could be focused only on features that are unique to this set. We exploit this intuition and make the following novel contributions:

- **Problem Formulation:** We formulate the problem of *domain-agnostic*, *labeled* graph generative modeling *under data scarcity*. To the best of our knowledge, we are the first to investigate this problem.
- **Algorithm:** We propose GSHOT, that effectively integrates meta-learning with auto-regressive graph generative model to facilitate transfer of knowledge from a set of auxiliary graph datasets to target graph dataset(s). Meta-learning on these auxiliary datasets fosters a high quality parameter initialization. Subsequently, using a *self-paced* fine-tuning approach, GSHOT adapts to unseen target graph dataset using a small number of training samples.
- **Empirical Evaluation:** We perform extensive experiments across multiple real labeled graph datasets spanning a variety of domains such as chemical compounds, proteins, and physical interaction systems. We establish that GSHOT is effective in learning graph distributions with high fidelity even on datasets containing as few as 50 training samples, and significantly improves over baselines that learn from scratch.

2 Problem Formulation [3]

Definition 1 (Graph)**.** *A graph is represented as $G = (V, E)$, where $V = \{v_1, \cdots, v_n\}$ is a set of n nodes and $E = \{(v_i, v_j) \mid v_i, v_j \in V\}$ is a set of edges. Let $\mathbb{L}_{node} : V \rightarrow \mathbb{V}$ and $\mathbb{L}_{edge} : E \rightarrow \mathbb{E}$ be the node and edge label mappings respectively where $\mathbb{V}$ and $\mathbb{E}$ are the set of all node and edge labels respectively. We assume that the graph is connected and there are no self-loops.*

A *graph dataset* D=$\{G_1, \cdots, G_N\}$ is a collection of N graphs. Graph dataset D_1 is considered to be an *auxiliary* dataset of graph dataset D_2 if D_1 is *similar* to D_2. As discussed in Sec. 1, a generic set of chemical compounds may be considered as an auxiliary dataset to a specific subgroup of compounds that display a desired activity against a virus. In the current context of *labeled domain-agnostic* graph generative modeling, we below define the concept of *graph dataset distance metric* and subsequently formally define *auxiliary dataset*.

Definition 2 (Graph Dataset Distance Metric)**.** *A graph dataset distance metric is a function $\Lambda_m(D_i, D_j) \mapsto \mathbb{R}$ that takes two graph datasets D_i and D_j as input and computes distance between the two datasets as per metric Λ_m.*

Several metrics have been proposed in the literature for comparing graph datasets [2, 13]. In Sec. 4.1 we describe various distance metrics.

[3] All notations used in our work are summarized in Table 2 in the appendix.

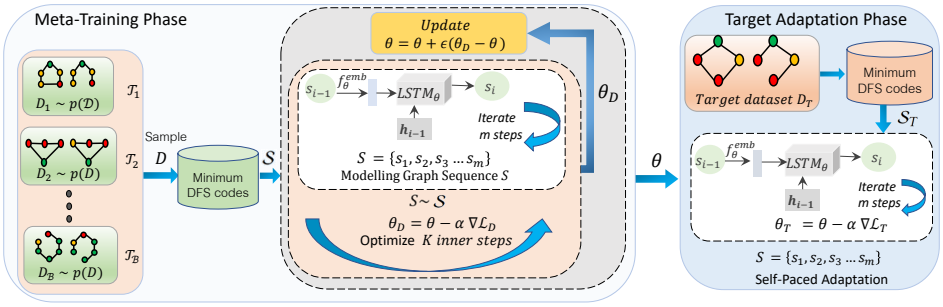

Figure 2: Architecture of GSHOT

Definition 3 (Auxiliary Dataset)**.** *A graph dataset is considered to be an auxiliary dataset to a target dataset if it satisfies the following conditions:*

1. *The node/edge label space of the target and auxiliary datasets should be similar.*
2. *The distances between auxiliary and target graph datasets should be low as per Defn. 2.*[4]

Problem 1 (Graph Generative modelling)**.** *The goal of labeled graph*[5] *generative modeling of a dataset D of graphs is to learn a model, $p_\theta(D)$, parameterized by θ, that approximates the true latent distribution $p(D)$ of graphs in D. The learned generative model is effective if it is capable of generating graphs similar to those in D.*

The goal is to learn a generative model over a target graph dataset D_T, where $|D_T|$ is small. Since $|D_T|$ is small, accurate modeling is hard (Recall Fig. 1a). However, if D_T is accompanied with a collection of auxiliary datasets, the generative model should be able to use this knowledge and augment its learning. Formally, it is defined as follows.

Problem 2 (Labeled Graph Generative Modelling under Data Scarcity)**.**
Input: *A collection of auxiliary graph datasets $\mathcal{D}=\{D_1, \cdots, D_\mathcal{B}\}$ and a target dataset D_T.*
Goal: *To learn a graph generative model $p_\theta(D)$ that is capable of leveraging the knowledge from $\mathcal{D}$ and effectively adapting to the unseen target dataset D_T.*

3 GSHOT: Proposed Methodology

Given a set of auxiliary datasets $D_1, \cdots, D_\mathcal{B}$, first, GSHOT learns *initial* model parameters θ. θ is learned in a strategic manner such that, at inference time, when an *unseen target dataset* D_T containing a small number of graphs are provided as input, we can fine-tune θ to new θ_T where $p_{\theta_T}(D_T)$ best approximates the true distribution of D_T. Finally, to generate graphs, we sample from $p_{\theta_T}(D_T)$. Fig. 1b provides a visual summary of this approach.

The proposed approach draws inspiration from *meta-learning* [21, 22]. The main objective of meta-learning is to learn initial model parameters for a set of *tasks* in such a way that they can be adapted to various unseen target *tasks* having limited training data. In the context of our problem, each task $\mathcal{T}_i$ refers to the graph generative modeling task for dataset D_i in the auxiliary dataset $\mathcal{D}$. Each task $\mathcal{T}_i$ is associated with a loss function $\mathcal{L}_i$. During meta-training, the optimal initial parameter θ is learned using $\mathcal{D}$. Then, given an *unseen target task* $\mathcal{T}_T$ corresponding to *unseen graph dataset* D_T with an associated loss $\mathcal{L}_T$, θ is fine-tuned for $\mathcal{L}_T$ using small number of data samples of $\mathcal{T}_T$. When mapped to our problem of graph generative modeling, the loss function measures how well $p_{\theta_T}(D_T)$ mimics the true distribution of D_T.

3.1 Architecture Overview

Fig. 2 presents the architecture of GSHOT. In order to learn a generative model over labeled graphs on a dataset D, we first convert graphs to *sequences*. This conversion allows us to leverage the rich literature on *auto-regressive generative models*. Auto-regressive methods[2, 13] have obtained superior fidelity and high scalability on domain-agnostic graph generative modeling task. Two popular encoding schemes for encoding graphs into sequence are *BFS encoding* [13] and *DFS encoding* [2]. In our work, we choose *DFS encoding*. This choice is motivated by the observation that *minimum DFS codes*, which is an instance of DFS encoding, provides one-to-one mapping from graphs to sequences. In contrast, in BFS encoding, the same graph may have multiple sequence representations, and may be exponential in the worst case with respect to the graph size. Consequently, one-to-one

[4] In App Sec. I we present similarity results between datasets on several metrics.
[5] In our paper we use the keyword *graph* and *labeled graph* interchangeably

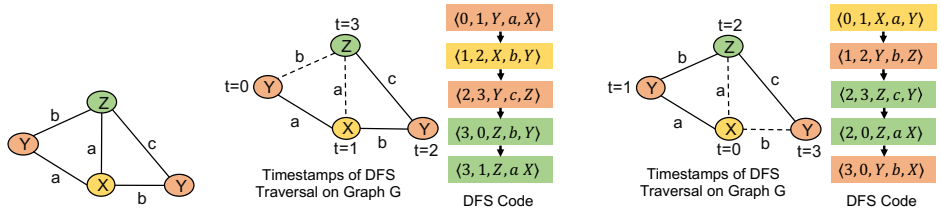

(a) Graph G **(b)** DFS Code 1 **(c)** DFS Code 2

Figure 3: Few possible DFS codes of graph G. DFS code 2 is smaller than DFS code 1 since $\langle 0, 1, X, a, Y \rangle$ is less than $\langle 0, 1, Y, a, X \rangle$

mapping is an attractive feature that our model can exploit, and as others have shown, it also improves the scalability and fidelity of graph generative modeling [2].

Once graphs are converted into sequences via *minimum DFS codes*, as shown in Fig. 2, *meta-learning* is conducted on the sequence representations to learn parameter set θ. To model sequences, we use LSTM as shown in Fig. 2. Finally, during target-adaptation phase, the target graph database D_T is converted to the equivalent sequence representation $\mathcal{S}_T$, followed by fine-tuning to learn θ_T. To generate graphs, we sample sequences from $p_{\theta_T}(\mathcal{S}_T)$, which are then converted to graphs. The conversion back from a sequence to its graph representation is trivial since our DFS-encoding enables one-to-one mapping. Hence, this conversion can be performed in $O(|E|)$ time, where E is the set of edges. We next deep-dive into each of these individual steps.

3.2 DFS Codes: Graph to Sequence encoding

We first formalize the concept *Graph Canonization*.

Definition 4 (Graph Isomorphism)**.** *Two graphs $G_i = (V_i, E_i)$ and $G_j = (V_j, E_j)$ are said to be isomorphic if there exists a bijection ϕ such that for every vertex $v \in V_i$, $\phi(v) \in V_j$ and for every edge $e = (u, v) \in E_i, \phi(e) = (\phi(u), \phi(v)) \in E_j$. Furthermore, for labeled graphs to be isomorphic, in addition to above conditions, the labels of mapped nodes and edges should be same, i.e., $\mathbb{L}_{node}(v) = \mathbb{L}_{node}(\phi(v))$ and $\mathbb{L}_{edge}(e) = \mathbb{L}_{edge}(\phi(e))$.*

Definition 5 (Graph Canonization)**.** *Graph canonization refers to the process of converting a graph into a label such that graphs have the same label if and only if they are isomorphic to each other. A label that satisfies this criteria is called a canonical label.*

Now, we introduce *minimum DFS codes* and how it corresponds to canonical labels of graphs. *DFS code* [23] is a mapping function defined over a graph G, which encodes G into a sequence of edge tuples. To construct a DFS-code from G, first, a depth-first search (DFS) traversal is started from an arbitrary node. During this traversal, a timestamp is assigned to each node based upon when it is discovered. The first discovered node is assigned timestamp 0, the second discovered node is assigned 1, and so on. Following these timestamps, each edge (u, v) is assigned a tuple of five items $\langle t_u, t_v, L_u = \mathbb{L}_{node}(u), L_{uv} = \mathbb{L}_{edge}(uv), L_v = \mathbb{L}_{node}(v) \rangle$. t_u, t_v are the discovery times of node u and v respectively. L_u, L_v and L_{uv} are labels of node u, node v and edge (u, v) respectively.

A partition of edges is created based upon the DFS traversal. The first partition consists of *forward edges* that are traversed by the DFS traversal. The second partition contains *backward edges*, that are not traversed during the DFS traversal. For example, in Fig. 3b, 3c, the edges depicted by solid lines depict the forward edges, and the one's which are dashed depict backward edges. A *total ordering* is imposed on these edges following the rules described in GSPAN [23] to obtain the DFS code of a graph. Specifically, for ordering forward edges, the process is straight forward. Forward edges are ordered based upon their discovery time in the DFS traversal. For backward edges, the ordering is derived based upon the following rules:

- Backward edge (u, s) must appear before all forward edges of the form (u, t).
- Backward edge (u, s) must appear after the forward edges of the form (t, u), i.e the first forward edge which points to u.
- For backward edges of the form (u, s) and (u, s') originating from the same source u, (u, s) is ordered before (u, s') if $t_s < t'_s$.

Fig. 3 shows examples of two DFS codes of a graph based on two DFS traversals. For more details on DFS code, we refer to GSPAN[23].

Minimum DFS codes: As shown in Fig.3, a graph can have multiple DFS codes. We choose the lexicographically smallest DFS code among all DFS codes as the *minimum* DFS code. It has been shown that there exists a *bijection* between a graph and its minimum DFS code [23]. Hence, minimum

DFS codes are canonical labels. Using minimum DFS codes, we encode each graph $G = (V, E)$ in dataset D as a sequence of m edge tuples $S = (s_1, \ldots, s_m)$ where $m = |E|$ and each s_i is an edge tuple of the form $\langle t_u, t_v, L_u, L_{uv}, L_v \rangle$. We use the notation $\mathcal{F}(G) = S$ to denote the minimum DFS code S of graph G. Applying $\mathcal{F}$ on all graphs of dataset D, we obtain a collection of edge tuple sequences $\mathcal{S} = \{\mathcal{F}(G) \mid \forall G \in D\}$ for all graphs in dataset D.

Computation Complexity: We note that computing the minimum DFS code of a graph is equivalent to performing graph isomorphism tests. In the literature, no polynomial time algorithm exists for detecting graph isomorphism. Fortunately, for labeled graphs, it has been shown that minimum DFS codes can be computed very efficiently[2, 23].

3.3 Modeling Graph Sequences

Minimum DFS codes are of sequential nature. We model each sequence $S{=}(s_1, \cdots, s_m)$ using an *auto-regressive* model[2] as follows:

$$p(S) = p(s_0) \prod_{i=1}^{m+1} p(s_i | s_0, \cdots, s_{i-1}) \tag{1}$$

where $m{=}|E|$ is the number of edges, s_0 is a *start-of-sequence* SOS token and s_{m+1} is *end-of-sequence* EOS token to allow variable length sequences. To learn the parameters for these sequential conditional distributions, we use *Recurrent Neural Networks*. Specifically, we use LSTM [24], which efficiently models long-range dependencies. Formally,

$$\mathbf{h}_i = LSTM_\theta^{hidden}\left(\mathbf{h}_0, \left(f_\theta^{emb}(s_0) \ldots f_\theta^{emb}(s_{i-1})\right)\right) \quad = LSTM_\theta^{hidden}\left(\mathbf{h}_{i-1}, f_\theta^{emb}\left(s_{i-1}\right)\right) \tag{2}$$

where $LSTM_\theta$ is a function representing an LSTM cell. f_θ^{emb} is an embedding function that takes *one-hot encoding* of s_{i-1} as input and produces a d-dimensional compressed vector. $\mathbf{h}_0$ is initialized to $\mathbf{0}$. Finally, assuming that $s_i.t_u$, $s_i.t_v$, $s_i.L_u$, $s_i.L_{uv}$, $s_i.L_v$ are independent[6] given $\mathbf{h}_i$, we predict $s_i = \langle t_u, t_v, L_u, L_{uv}, L_v \rangle$ as follows.

$$\widetilde{s}_i = \left\langle f_\theta^{t_u}(\mathbf{h}_i), f_\theta^{t_v}(\mathbf{h}_i), f_\theta^{L_u}(\mathbf{h}_i), f_\theta^{L_{uv}}(\mathbf{h}_i), f_\theta^{L_v}(\mathbf{h}_i) \right\rangle \tag{3}$$

where each f_θ is a function representing a fully connected *Multi-layered Perceptron (MLP)*. Note that every function in this discussion is parameterized by θ (indicated by the subscript). Finally, we define the loss $\mathcal{L}_D$ specific to sequence (graph) generation task $\mathcal{T}_D$ on dataset D as follows:

$$\mathcal{L}_S = -\sum_{i=1}^{m+1} \sum_{c} \left(s_i[c] \log \widetilde{s}_i[c] + (1 - s_i[c]) \log\left(1 - \widetilde{s}_i[c]\right)\right) \quad , \quad \mathcal{L}_D = \sum_{S \in \mathcal{S}} \mathcal{L}_S \tag{4}$$

Here c is the component index of one-hot vector s_i and predicted vector $\widetilde{s}_i$. $\mathcal{S}$ is the collection of graph sequences S derived by encoding every graph $G{\in}D$ using minimum DFS coding function $\mathcal{F}(G)$.

3.4 Meta-Learning for Labeled Graph Generative Modeling under limited availabiltiy of data

Up until now, we have defined parameters θ of graph generative model $p_\theta(D)$. As motivated, we want to find an initialization of θ such that it can quickly learn to generate graphs from unseen dataset D_T having small number of training graph samples. Specifically, we train θ on graphs from auxiliary datasets to learn initial parameters. To do this, we build upon the REPTILE framework [25]. REPTILE is a *first-order* meta-learning algorithm, wherein it uses first-order gradients to learn θ, and is therefore computationally and memory efficient. GSHOT, using REPTILE, extracts the *meta-knowledge* to obtain an effective initialization and an ability to adapt to the target dataset using limited fine-tuning samples. More concretely, GSHOT optimizes the below objective function in order to learn good initialization of θ:

$$\min_\theta \mathbb{E}_{\mathcal{L}_{D \sim \mathcal{D}}} \left[\mathcal{L}_D(\theta_D^K)\right], \tag{5}$$

where θ_D^K are the updated parameters after K gradient updates of θ from dataset D as follows:

$$\theta^0 = \theta \quad \text{and} \qquad \theta_D^i = \theta_D^{i-1} - \alpha \nabla_{\theta^{i-1}} \mathcal{L}_D \quad \forall i \in [1 \ldots K] \tag{6}$$

Here hyper-parameter α controls the meta-learning rate. Finally using the K step updated parameters θ_D^K, we optimize Eq. 5 as follows:

$$\theta = \theta + \epsilon\left(\theta_D^K - \theta\right) \tag{7}$$

where ϵ and K are hyper-parameters of GSHOT. Eq. 7 updates the value of the meta-parameters θ using a weighted combination of θ and *K-step* fine-tuned parameter θ_D^K for dataset D. The parameter ϵ can be considered as a step-size in the direction of the gradient $\theta_D^K - \theta$. We iterate over $D{\sim}\mathcal{D}$ by computing Eq. 6 for different tasks and then using it for optimizing Eq. 5. Algorithm 1 in App. describes the pseudocode of meta-training procedure of GSHOT.

[6] In Sec. G in Appendix, we study the impact of predicting the components of edge tuple conditionally instead of independently.

3.5 Adaptation to Target Dataset

Once GSHOT is meta-trained on diverse graph datasets, our next goal is to adapt the learned model parameters to the target dataset D_T. Essentially, first we initialize the target model parameters to the value of the meta-trained model:

$$\theta_T = \theta \tag{Initialization}$$

Towards our goal to optimize parameters on the target dataset, a simple approach is to update the parameters of the model by applying multiple gradient updates using samples from target dataset D_T with its associated loss as follows:

$$\theta_T = \theta_T - \alpha \nabla_{\theta_T} \mathcal{L}_T \tag{gradient updates}$$

The above equation assumes, for every gradient update, the training data is sampled in a random fashion from the target dataset. However, recent studies have discovered that gradually increasing the complexity of training instances results in better learning and faster convergence [26]. Motivated by this result, we adopt *self-paced learning* [27] in the fine-tuning phase of GSHOT. Towards this end, we modify the loss $\mathcal{L}_T$ associated with the target dataset in a way that the model is presented with training samples of gradually increasing difficulty. Moreover, the training curriculum is dynamically determined by the model itself based upon its *perception* of the difficulty of a sample. Specifically, recall from Eq. 4 $\mathcal{L}_D = \sum_{S \in \mathcal{S}} \mathcal{L}_S$ where $\mathcal{S}$ is the collection of graph sequences of $G \in D$. For self-paced learning, we modify $\mathcal{L}_T$ as follows:

$$\mathcal{L}_T = \sum_{i=1}^{|\mathcal{S}_T|} \beta_i \mathcal{L}_{S_i} - \lambda \sum_{i=1}^{|\mathcal{S}_T|} \beta_i \qquad \beta_i \in \{0,1\} \;\; \forall i \in [1 \ldots |\mathcal{S}_T|] \tag{8}$$

where $\mathcal{S}_T = \{\mathcal{F}(G) \mid \forall G \in D_T\}$, $S_i \in \mathcal{S}_T$, and $|\mathcal{S}_T|$ is the number of graphs in D_T. λ is an evolving parameter that essentially controls the pace of learning. Specifically in our graph generative modeling setting, we solve this via an iterative approach [27]. Before every gradient update as described earlier, we first calculate the value of β_i's as follows:

$$\beta_i = \begin{cases} 1 & if \;\; \mathcal{L}_{S_i} < \lambda \\ 0 & else \end{cases} \tag{9}$$

The value of β_i indicates whether the ith training sample will be used or not in the loss computation in Eq. 8 . We substitute these values in Eq. 8 and update the parameters θ_T. This process repeats until convergence. The value of λ, is increased periodically by a growth factor γ to gradually allow hard samples to be a part of the loss computation during the course of training. Algorithm 2 in App. describes the pseudocode of the fine-tuning procedure of GSHOT.

3.6 Graph Generation

After fine tuning $p_\theta(D)$ on target dataset D_T, we obtain $p_{\theta_T}(D_T)$. We sample graphs from this distribution as follows. First, we pass the initial hidden state $\mathbf{h}_0 = \mathbf{0}$ to $LSTM_{\theta_T}$ along with the SOS symbol. At each step i, we sample s_i from the updated hidden state $\mathbf{h}_i$ as follows-

$$s_i.t_u \sim \; Multinomial(f^{t_u}_{\theta_T}(\mathbf{h}_i)) \qquad s_i.t_v \sim \; Multinomial(f^{t_v}_{\theta_T}(\mathbf{h}_i))$$

$$s_i.L_u \sim \; Multinomial(f^{L_u}_{\theta_T}(\mathbf{h}_i)) \qquad s_i.L_{uv} \sim \; Multinomial(f^{L_{uv}}_{\theta_T}(\mathbf{h}_i)) \tag{10}$$

$$s_i.L_v \sim \; Multinomial(f^{L_v}_{\theta_T}(\mathbf{h}_i)) \tag{11}$$

The process is repeated until the EOS symbol is sampled for any of the five components in the sampled tuple. Finally, this sampled sequence, representing the DFS code, is converted back to graph. Algorithm 3 in App. presents the pseudocode of the graph generation phase.

4 Experiments

We benchmark GSHOT against state-of-the-art algorithms for graph generation and establish that:

- **Higher fidelity:** GSHOT generates graphs of higher fidelity than the state-of-the-art methods.
- **Sample-efficient:** Attributed to its capability to learn with a limited amount of data, GSHOT better preserves graph properties compared to existing methods even when the number of fine-tuning samples used by GSHOT are relatively less compared to other methods.

The code to reproduce the experiments can be found at `https://github.com/idea-iitd/GShot`.

4.1 Experimental setup

Datasets: Since our focus is on *domain-agnostic labeled* graph generative modeling, we show the effectiveness of our proposed approach using datasets from diverse domains. Moreover, in our experiments, we use target datasets having significantly low volumes of available graphs in comparison to other works in literature [2, 6, 13, 28]. Table 3 in App. C summaries the different datasets. Further details on semantics of the datasets are also present in App. C.

Train-test splits: We briefly describe our datasets' train-test split.

- **Biological Domain:** Each enzyme in the Enzyme dataset[11] belongs to one of six classes, namely EC1, EC2, EC3, EC4, EC5, EC6. We treat enzymes in EC1, EC2, EC4, EC5, EC6 as auxiliary datasets and EC3 as our target dataset, which consists of 100 enzymes. [7]
- **Chemical Domain:** We use anti-cancer screen datasets *Yeast*, *Breast*, and *Lung* as auxiliary datasets for meta-training and use the two smallest chemical datasets of *AIDS-CA* and *Leukemia-Active* as our target set.
- **Physics Domain:** We meta-train GSHOT on auxiliary datasets consisting of *four* and *six* particle spring systems and then fine-tune on graphs containing *five* particles.

Baselines: We benchmark the performance of GSHOT against the state-of-the-art techniques for *domain-agnostic, labeled* graph generative modeling, namely GRAPHGEN [2] and GRAPHRNN [13]. We do not include GRAN[6] as a baseline since it cannot generate labeled graphs. For GRAPHGEN, we used the code shared by authors. While, in theory, GRAPHRNN supports labeled graphs, the code shared by the authors do not. Hence, we extend the author's code as outlined in the supplementary section of GRAPHRNN [13]. Both GRAPHGEN and GRAPHRNN are trained *only* on the target dataset and we compare the quality of the generated graphs with that of GSHOT. This comparison allows us to evaluate how efficient the knowledge transfer of GSHOT is as opposed to relying only on the target dataset.

In addition, we use a third *pre-training* baseline introduced by us, which we will refer to as PRE-TRAIN+FT. In this baseline, we first pre-train GRAPHGEN on the same auxiliary datasets used by GSHOT for meta-training. Then, we fine-tune it on the target dataset. This baseline allows us to systematically understand the impact of meta-learning against generic generative modeling. We do not consider pre-training on GRAPHRNN, since GRAPHGEN has been shown to be superior on the labeled graph generative modeling task [2], which is also reflected in our experiments that follows.

Evaluation setup: During meta-training of GSHOT, we use $\approx 50\%$ data for training and the same for validation. During fine-tuning to a new graph dataset, unless specifically mentioned, we use the default split among training, validation, and test as $\approx 40\%$, $\approx 30\%$, and $\approx 30\%$ respectively. Unless specified otherwise, for training a model from scratch directly on the target dataset or fine-tuning a model on a target dataset, we use the same number of training samples of the target dataset. For each target dataset, this information is present in the *#Target Training samples* column of Table 1. The system configuration and parameter details can be found in App. D.

Evaluation Metrics: The performance of a graph generative model is satisfactory **(1)** if it generates graphs with similar properties as the source graphs, **(2)** but without duplicating the source graphs themselves. To quantify these, we divide our metrics into two categories.

- **Fidelity:** To quantify the preservation of graph properties, we compare the distributions of graph statistics between the ground truth graphs and the generated graphs using the following metrics.
  - **Structural metrics:** To quantify the preservation of original graph properties, we use the structural metrics used by GraphRNN and GraphGen: **(1)** *node degree distribution* (Degree), **(2)** *clustering coefficient distribution of nodes* (Clustering), and **(3)** *orbit count distribution* (Orbit) [29], which measures the number of orbits with 4 nodes. This metric captures the higher-level motifs that are shared between generated and test graphs. We utilize *Maximum Mean Discrepancy (MMD)* [30] to compute the distance between two distributions. Further, to compare the sizes of the generated graphs against the ground truth, we measure **(4)** *Average node count* and **(5)** *Average edge count*.
  - **Labeled Graph Metrics:** Our work is geared towards labeled graph generation. Hence, it is important to assess whether a generative model captures the label distribution well. Towards that end, we compare the distribution of **(1)** Node Labels, **(2)** Edge Labels, and **(3)** the *joint*

[7] In Sec. I in Appendix we find similarity of target datasets with auxiliary datasets and show impact of performance of GSHOT using different auxiliary datasets having different similarity.

Table 1: Summary of performance by GSHOT, GRAPHGEN, GRAPHRNN, and PRETRAIN+FT baseline on different datasets on multiple metrics. Values less than 10^{-3} are approximated to 0. The best-performing model for each dataset is highlighted in bold.

Auxiliary datasets	Target dataset	#Target Training Samples	Model	Deg.	Clus.	Orbit	NSPDK	Avg # Nodes (Gen/Gold)	Avg # Edges (Gen/Gold)	Node Label	Edge Label	Joint Node Label & Degree	Novelty	Uniqueness
Enzyme: EC1,EC2, EC4,EC5, EC6	Enzyme: EC3	50	GRAPHGEN	0.90	0.58	0.127	0.266	17.51/26.90	22.22/52.85	0.015	x	0.714	**100%**	**100%**
			GRAPHRNN	**0.30**	0.73	0.13	0.214	20.51/26.90	36.23/52.85	0.019	x	0.696	**100%**	**100%**
			PRETRAIN+FT	0.72	0.63	0.053	0.18	23.73/26.90	33.2/52.85	0.0095	x	0.619	99%	99%
			GSHOT	0.45	**0.47**	**0.025**	**0.16**	**24.5/26.90**	**37.69/52.85**	**0.004**	x	**0.457**	**100%**	**100%**
Yeast, Breast, Lung	AIDS-CA	150	GRAPHGEN	0.026	0.016	0.003	0.127	17.51/37.14	17.62/39.60	0.05	0.001	0.20	98%	97%
			GraphRNN	0.15	0.47	0.045	0.14	**30.5/37.14**	**40.19/39.60**	0.193	0.005	0.836	86%	45%
			PRETRAIN+FT	0.021	0.004	≈ 0	0.11	24.1/37.14	25.22/39.60	0.013	$\approx$ **0**	0.173	**99%**	**99%**
			GSHOT	**0.017**	**0.0015**	$\approx$ **0**	**0.08**	26.5/37.14	27.1/39.60	**0.011**	$\approx$ **0**	**0.14**	**99%**	**99%**
	Leukemia-Active	500	GRAPHGEN	0.06	0.019	≈ 0	0.17	40.02/47.71	42.23/50.37	0.02	$\approx$ **0**	0.99	**100%**	**100%**
			GraphRNN	0.06	0.554	0.032	0.34	7.17/47.71	7.51/50.37	0.39	0.017	0.83	**100%**	**100%**
			PRETRAIN+FT	0.039	0.0064	≈ 0	0.116	**43.08/47.71**	**45.5/50.37**	0.09	$\approx$ **0**	0.79	98%	98%
			GSHOT	**0.0069**	$\approx$ **0**	$\approx$ **0**	**0.032**	42.35/47.71	44.33/50.37	**0.0011**	$\approx$ **0**	**0.24**	**100%**	**100%**
{4, 6} body Spring	5-body Spring	500	GRAPHGEN	**0.004**	**0.015**	$\approx$ **0**	**0.016**	**4.98/5**	**5.49/5.64**	0.012	x	**0.011**	33%	13%
			GraphRNN	0.018	0.012	$\approx$ **0**	0.029	4.71/5	5.03/5.64	0.044	x	0.017	**87%**	**55%**
			PRETRAIN+FT	0.021	0.047	0.0025	0.017	**4.98/5**	5.19/5.64	**0.011**	x	0.012	70%	49%
			GSHOT	0.008	0.035	$\approx$ **0**	**0.016**	**4.98/5**	5.38/5.64	0.016	x	0.012	64%	41%

distribution of node labels and degree in the ground truth and generated graphs. We again use MMD to quantify the distance from the ground truth.

- **Topological Similarity:** Finally, in order to capture topological similarity of generated graphs with the ground truth graphs, we use *Neighbourhood Sub-graph Pairwise Distance Kernel (NSPDK)* [31]. NSPDK provides the benefit of incorporating both node and edge labels along with the structure of the graph. Specifically, NSPDK measures the distance between two graphs by matching pairs of subgraphs with different radii and distances. The lower the MMD score for NSPDK, the more aligned are the two graph distributions.

- **Duplication and Uniqueness:** A model that generates graphs with high fidelity might not be useful in practice unless it is also capable of generating graphs that are not seen in the training data. In order to capture this requirement, we utilize the below metrics introduced by GRAPHGEN [2]: **(1)** *Novelty* measures the percentage of generated graphs that are not subgraphs of the set of the training graphs. Additionally, we compute **(2)** *Uniqueness*, which captures the diversity of the set of generated graphs. In order to quantify uniqueness, we remove the generated graphs that are subgraph isomorphic to any of the other generated graphs. This is different from the novelty metric as here we focus only on the generated graphs. A model that generates 100 graphs and out of which 90 are subgraph isomorphic to any of the other generated graphs has uniqueness$=10\%$.

In order to quantify the quality of a particular metric, we generate multiple graphs for each target dataset and compare them against the available ground truth target graphs. Details of number of graphs generated for each dataset is present in App. D.2.

4.2 Quality

Fidelity: Table 1 shows the performance of all the models across different datasets. We observe that, in most cases, GSHOT obtains lower MMD scores compared to baselines. In terms of the global level graph metric *NSPDK*, GSHOT achieves a significant improvement even against the best performing baselines. For instance in Leukemia-Active, for *NSPDK*, GSHOT obtains MMD value of 0.032 against a significantly higher value of 0.116 obtained by PRETRAIN+FT. With respect to labeled graph metrics, we observe that GSHOT improves over state-of-the-art techniques by achieving more than 50% lower MMD value in multiple cases. Further, GSHOT also outperforms existing techniques in the *Joint Node-Label and Degree* metric signifying its ability to better jointly model the graph structure and labels. While GSHOT achieves high quality on most fidelity metrics, however on the node/edge count metric when the number of fine-tuning graphs becomes very low(Eg:- Enzyme EC3 = 50 and AIDS-CA = 150), its performance deteriorates for this metric. We would also like to highlight that modeling the edge tuple conditionally in GSHOT (see App G), improves this metric to a certain extent on all datasets. Among all baselines only GRAPHRNN's performance on AIDS-CA for avg node/edge count is superior to GSHOT, however it performs worser on other fidelity metrics . Having said that, the superior performance of GSHOT establishes the efficacy of the meta-training procedure to learn an effective set of initial model parameters, which adapts well to low-data regimes.

Uniqueness and novelty: In addition to obtaining better fidelity in most cases, GSHOT also achieves a higher or similar score compared to baselines on the *Novelty* and *Uniqueness* aspect. On AIDS-CA dataset, we obtain an improvement of $\approx 1-2\%$ in the uniqueness and novelty metrics against GRAPHGEN while also achieving better fidelity scores. Additionally, for AIDS-CA, GRAPHRNN's performance in terms of both fidelity as well as diversity is significantly inferior to other methods. In the case of the 5-body spring dataset, although GSHOT does not perform the best in terms of

fidelity scores, still its uniqueness and novelty scores are significantly higher than GRAPHGEN, which achieves a 33% novelty score and 13% uniqueness score. This indicates that GRAPHGEN mostly generated duplicated graphs. In context of Physics dataset, we highlight that the target graphs are extremely small i.e having only 5 nodes. It is more challenging to generate unique and diverse graphs in this context when compared to datasets belonging to other category such as chemical/biological where graphs are large. We observe that only GraphRNN is able to generate graphs which are more novel and unique, however, its performance is significantly poor on all fidelity metrics. Overall, we observe that an efficient parameter initialization obtained by GSHOT also helps in improving the diversity of generated graphs while generating graphs with high fidelity.

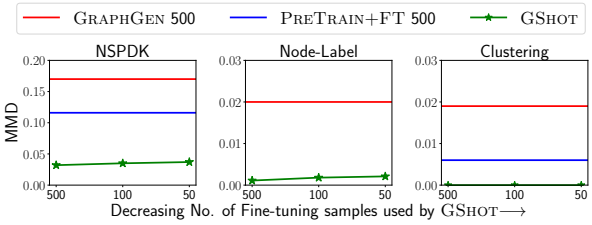

Figure 4: The variation in MMD scores on different metrics when the number of fine-tuning samples for GSHOT is reduced from 500 to 50 on the Leukemia-Active dataset. Here the suffix of 500 after GRAPHGEN and PRETRAIN+FT depicts that the number of training samples used from the target dataset for these baselines is 500. Note that for PRETRAIN+FT 500, the value of the Node-Label metric (0.09) was skipped in the diagram to improve readability.

Robustness to number of fine-tuning samples: We also evaluate GSHOT's robustness to different sizes of the same fine-tuning dataset. Towards this end, we choose Leukemia-Active dataset as our target dataset since due to slightly higher availability of fine-tuning data, there is a reasonable scope to down-sample the fine-tuning data in order to understand its impact on performance. We vary the number of fine-tuning samples available to GSHOT from 500 to 50. However, we keep the number of fine-tuning samples for the baselines to the maximum value, i.e., 500. In Fig. 4, we observe that GSHOT, while using less number of samples from the target dataset, still obtains lower MMD scores on different metrics in comparison to GRAPHGEN and the PRETRAIN+FT model that used 500 samples from the target dataset. Further, the MMD scores for GSHOT increase only slightly when the number of fine-tuning samples is reduced from 500 to 50. This is a direct consequence of our model's ability to adapt with a small number of training samples. Further, we would like to highlight that the novelty and uniqueness metrics did not show any observable change in this experiment.

Ablation study: We study the improvement obtained by using *self-paced fine-tuning* in GSHOT over *vanilla fine-tuning* in Appendix E. In App. F, we study the impact of the choice of auxiliary datasets on the performance of graph generative modeling under data scarcity.

5 Conclusion

Research on deep graph generative modeling has progressed significantly in several directions such as scalability to large graphs, domain agnostic modeling, handling node and edge labels, etc. However, the problem of learning to generate graphs in low-data regimes remained unexplored. In this work, we propose the paradigm of *domain-agnostic, labeled graph generative modeling under data scarcity*. Our proposed architecture GSHOT learns to transfer meta-knowledge from auxiliary graph datasets to a target dataset. Utilizing these prior experiences, GSHOT quickly adapts to an unseen graph dataset through *self-paced fine-tuning*. GSHOT is effective in learning graph distributions on datasets with small number of available training samples. Extensive evaluation on real graph datasets demonstrate that graphs generated by GSHOT preserve graph structural properties significantly better than the state-of-the-art approaches. Although, our proposed method outperforms existing state-of-the-art methods, however, while generating these molecules, it does not take into account their molecular/chemical properties etc. In future, we would like to work on capturing these aspects.

6 Acknowledgement

Srikanta Bedathur was partially supported by a DS Chair of AI fellowship. Sayan Ranu acknowledges the Nick McKeown chair position endowment. Sahil Manchanda was partially supported by Qualcomm Innovation Fellowship.

References

[1] Jiaxuan You, Bowen Liu, Rex Ying, Vijay Pande, and Jure Leskovec. Graph convolutional policy network for goal-directed molecular graph generation. In *NeurIPS*, NIPS'18, page 6412–6422, Red Hook, NY, USA, 2018. Curran Associates Inc. 1

[2] Nikhil Goyal, Harsh Vardhan Jain, and Sayan Ranu. Graphgen: a scalable approach to domain-agnostic labeled graph generation. In *Proceedings of The Web Conference 2020*, pages 1253–1263, 2020. 1, 2, 3, 4, 5, 7, 8

[3] Nicola De Cao and Thomas Kipf. MolGAN: An implicit generative model for small molecular graphs. *ICML 2018 workshop on Theoretical Foundations and Applications of Deep Generative Models*, 2018.

[4] Aleksandar Bojchevski, Oleksandr Shchur, Daniel Zügner, and Stephan Günnemann. Netgan: Generating graphs via random walks. In *Proceedings of the 35th International Conference on Machine Learning, ICML 2018, Stockholmsmässan, Stockholm, Sweden, July 10-15, 2018*, pages 609–618, 2018.

[5] Réka Albert and Albert-László Barabási. Statistical mechanics of complex networks. *Reviews of modern physics*, 74(1):47, 2002.

[6] Renjie Liao, Yujia Li, Yang Song, Shenlong Wang, Charlie Nash, William L. Hamilton, David Duvenaud, Raquel Urtasun, and Richard Zemel. Efficient graph generation with graph recurrent attention networks. In *NeurIPS*, 2019. 7

[7] Martin Simonovsky and Nikos Komodakis. Graphvae: Towards generation of small graphs using variational autoencoders. In Vera Kurková, Yannis Manolopoulos, Barbara Hammer, Lazaros S. Iliadis, and Ilias Maglogiannis, editors, *Artificial Neural Networks and Machine Learning - ICANN 2018*, volume 11139 of *Lecture Notes in Computer Science*, pages 412–422, 2018.

[8] Shubham Gupta, Sahil Manchanda, Srikanta Bedathur, and Sayan Ranu. Tigger: Scalable generative modelling for temporal interaction graphs. In *Proceedings of the AAAI Conference on Artificial Intelligence*, volume 36, pages 6819–6828, 2022.

[9] Shubham Gupta and Srikanta Bedathur. A survey on temporal graph representation learning and generative modeling, 2022.

[10] Jayant Jain, Vrittika Bagadia, Sahil Manchanda, and Sayan Ranu. Neuromlr: Robust & reliable route recommendation on road networks. *Advances in Neural Information Processing Systems*, 34:22070–22082, 2021. 1

[11] Karsten M. Borgwardt, Cheng Soon Ong, Stefan Schönauer, S. V. N. Vishwanathan, Alexander J. Smola, and Hans-Peter Kriegel. Protein function prediction via graph kernels. *Bioinformatics*, 21 Suppl 1:i47–56, 2005. 1, 7, 15

[12] U.S. National Library of Medicine National Center for Biotechnology Information. Pubchem. URL `http://pubchem.ncbi.nlm.nih.gov`. 1, 14, 15

[13] Jiaxuan You, Rex Ying, Xiang Ren, William L. Hamilton, and Jure Leskovec. Graphrnn: Generating realistic graphs with deep auto-regressive models. In *ICML, 2018*, volume 80 of *Proceedings of Machine Learning Research*, pages 5694–5703. PMLR, 2018. 1, 2, 3, 7

[14] Sergey Bartunov and Dmitry Vetrov. Few-shot generative modelling with generative matching networks. In *International Conference on Artificial Intelligence and Statistics*, pages 670–678. PMLR, 2018. 1

[15] David C Swinney and Shuangluo Xia. The discovery of medicines for rare diseases. *Future medicinal chemistry*, 6(9):987–1002, 2014. 1

[16] Wen Cui, Kailin Yang, and Haitao Yang. Recent progress in the drug development targeting sars-cov-2 main protease as treatment for covid-19. *Frontiers in Molecular Biosciences*, 7, 2020. ISSN 2296-889X. 1

[17] Thomas Kipf, Ethan Fetaya, Kuan-Chieh Wang, Max Welling, and Richard Zemel. Neural relational inference for interacting systems. In *International Conference on Machine Learning*, pages 2688–2697, 2018. 1, 14

[18] Nathanaël Perraudin, Ankit Srivastava, Aurelien Lucchi, Tomasz Kacprzak, Thomas Hofmann, and Alexandre Réfrégier. Cosmological n-body simulations: a challenge for scalable generative models. *Computational Astrophysics and Cosmology*, 6(1):1–17, 2019.

[19] Yuanqi. Graphgt: Machine learning datasets for graph generation and transformation. In *Thirty-fifth Conference on Neural Information Processing Systems Datasets and Benchmarks Track (Round 2)*, 2021. 1, 14, 15

[20] John J Irwin and Brian K Shoichet. Zinc- a free database of commercially available compounds for virtual screening. *Journal of chemical information and modeling*, 45(1):177–182, 2005. 2

[21] Chelsea Finn, Pieter Abbeel, and Sergey Levine. Model-agnostic meta-learning for fast adaptation of deep networks. In *International conference on machine learning*, pages 1126–1135. PMLR, 2017. 3

[22] Sahil Manchanda, Sofia Michel, Darko Drakulic, and Jean-Marc Andreoli. On the generalization of neural combinatorial optimization heuristics. In *Joint European Conference on Machine Learning and Knowledge Discovery in Databases*, pages 426–442. Springer, 2022. 3

[23] Xifeng Yan. gspan: Graph-based substructure pattern mining. In *Proceedings of the 2002 IEEE International Conference on Data Mining (ICDM 2002), 9-12 December 2002, Maebashi City, Japan*, pages 721–724, 2002. 4, 5, 14

[24] Sepp Hochreiter and Jürgen Schmidhuber. Long Short-Term Memory. *Neural Computation*, 9 (8):1735–1780, 11 1997. ISSN 0899-7667. 5

[25] Alex Nichol and John Schulman. Reptile: a scalable metalearning algorithm. *arXiv preprint arXiv:1803.02999*, 2(3):4, 2018. 5

[26] Wojciech Zaremba and Ilya Sutskever. Learning to execute, 2015. 6

[27] M. Kumar, Benjamin Packer, and Daphne Koller. Self-paced learning for latent variable models. In *NeurIPS*, volume 23. Curran Associates, Inc., 2010. 6

[28] Wataru Kawai, Yusuke Mukuta, and Tatsuya Harada. GRAM: scalable generative models for graphs with graph attention mechanism. *CoRR*, abs/1906.01861, 2019. 7

[29] Tomaž Hočevar and Janez Demšar. A combinatorial approach to graphlet counting. *Bioinformatics*, 30(4):559–565, 2014. 7

[30] Arthur Gretton, Karsten M. Borgwardt, Malte J. Rasch, Bernhard Schölkopf, and Alexander J. Smola. A kernel two-sample test. *J. Mach. Learn. Res.*, 13:723–773, 2012. 7

[31] Fabrizio Costa. Fast neighborhood subgraph pairwise distance kernel. In *ICML*, pages 255–262, 2010. 8

[32] John Ingraham, Vikas Garg, Regina Barzilay, and Tommi Jaakkola. Generative models for graph-based protein design. *Advances in Neural Information Processing Systems*, 32, 2019. 14

[33] Xiaojie Guo, Yuanqi Du, Sivani Tadepalli, Liang Zhao, and Amarda Shehu. Generating tertiary protein structures via an interpretative variational autoencoder. *arXiv preprint arXiv:2004.07119*, 2020. 14

[34] Ida Schomburg, Antje Chang, Christian Ebeling, Marion Gremse, Christian Heldt, Gregor Huhn, and Dietmar Schomburg. Brenda, the enzyme database: updates and major new developments. *Nucleic acids research*, 32 Database issue:D431–3, 2004. 14

[35] Ashish Vaswani, Noam Shazeer, Niki Parmar, Jakob Uszkoreit, Llion Jones, Aidan N Gomez, Ł ukasz Kaiser, and Illia Polosukhin. Attention is all you need. In I. Guyon, U. Von Luxburg, S. Bengio, H. Wallach, R. Fergus, S. Vishwanathan, and R. Garnett, editors, *Advances in Neural Information Processing Systems*, volume 30. Curran Associates, Inc., 2017. URL https://proceedings.neurips.cc/paper_files/paper/2017/file/3f5ee243547dee91fbd053c1c4a845aa-Paper.pdf. 17

7 Appendix

A Notations

Symbol	Meaning
$G = (V, E)$	A Graph with vertex set V and edge set E
n	Number of nodes in G
m	Number of edges in G
$\mathbb{V}$	Label set of vertices in G
$\mathbb{E}$	Label set of edges in G
D=$\{G_1, G_2, \cdots, G_N\}$	Dataset of N graphs
$\mathcal{D}$=$\{D_1, \cdots, D_{\mathcal{B}}\}$	Collection of $\mathcal{B}$ graph datasets
t_u	DFS discovery time of node u
t_v	DFS discovery time of node v
L_u	Label of node u
L_{uv}	Label of edge (u, v)
L_v	Label of node v
$\mathcal{F}(\mathcal{G})$	Function to map graph to Minimum DFS code S
$S = (s_1, s_2 \ldots s_m)$	Minimum DFS Codes of a graph
$\mathcal{S} = \{S_1, S_2 \cdots S_N\}$	Collection of Minimum DFS codes of a dataset with N graphs
$\mathcal{T}$	Set of graph generative modelling tasks
$\mathcal{T}_i$	Graph generative modelling task for the ith dataset
$\mathcal{L}_i$	Loss associated with dataset D_i
θ	Model parameters
D_T	Target graph dataset
$\mathcal{S}_T$	Collection of Minimum DFS codes for target dataset D_T
θ_T	Parameters fine-tuned to the dataset D_T
β_i	Binary loss coefficient for i^{th} sample in eq. 8
γ	Growth parameter in self-paced fine-tuning

Table 2: Notations used in the paper

B Pseudocodes

Algorithm 1: Pseudocode for meta-training phase of GSHOT

Input : Collection of $\mathcal{B}$ graph datasets $\mathcal{D} = \{D_1, D_2 \ldots D_{\mathcal{B}}\}$, K, ϵ
Output : Good initialization of parameters θ of generative model $p_\theta(D)$
Initialise meta-parameters θ randomly.
repeat
  Sample a dataset $D \in \mathcal{D}$
  $\mathcal{S} = \{S = \mathcal{F}(G) \mid \forall G \in D\}$ `// Get Minimum DFS code`
  $\theta_D \leftarrow \theta$ `// Dataset` D `specific parameters`
  for K *times* **do** `//` K `inner gradient steps`
    $S = [s_1, s_2 \ldots s_m] \sim \mathcal{S}$
    $s_0 \leftarrow$ SOS
    $h_0 \leftarrow \mathbf{0}$
    $\mathcal{L}_D \leftarrow 0$
    `/* Computing loss` $\mathcal{L}_D$ `of sequence` $S = [s_0, s_1, s_2 \ldots s_{m+1}]$ `*/`
    for i *from* 1 *to* $m+1$ **do** `//` s_{m+1} `for EOS tokens`
      $\mathbf{h}_i \leftarrow LSTM_\theta^{hidden}(\mathbf{h}_{i-1}, f_\theta^{emb}(s_{i-1}))$
      $\widetilde{s}_i \leftarrow \left\langle f_\theta^{tu}(\mathbf{h}_i), f_\theta^{tv}(\mathbf{h}_i), f_\theta^{Lu}(\mathbf{h}_i), f_\theta^{Luv}(\mathbf{h}_i), f_\theta^{Lv}(\mathbf{h}_i) \right\rangle$
      $\mathcal{L}_D \leftarrow \mathcal{L}_D + \sum_c (s_i[c] \log \widetilde{s}_i[c] + (1 - s_i[c]) \log (1 - \widetilde{s}_i[c]))$
    $\theta_D \leftarrow \theta_D - \alpha \nabla_{\theta_D} \mathcal{L}_D$ `// D specific parameters' update`
  Update $\theta \leftarrow \theta + \epsilon(\theta_D - \theta)$ `// Meta gradient update`
until *stopping criteria* `// Typically when validation loss is minimized`

Algorithm 2: Fine-tuning GSHOT on target dataset D_T

Input : Target dataset D_T, meta-trained parameters θ, batch size B, growth factor γ, λ
Output : Fine tuned parameters θ_T for target dataset D_T
$\mathcal{S}_\mathcal{T} = \{S = \mathcal{F}(G) \mid \forall G \in D_T\}$ `// Get Minimum DFS code`
$\theta_T \leftarrow \theta$ `// Initializing parameters specific to target dataset` D_T
repeat
  $\mathcal{L}_T \leftarrow 0$;
  for B *times* **do** `// Sample` B `graphs for every batch`
    $S = [s_1, s_2 \ldots s_m] \sim \mathcal{S}_\mathcal{T}$
    $s_0 \leftarrow$ SOS
    $h_0 \leftarrow \mathbf{0}$
    $l \leftarrow 0$ `// Instance specific loss`
    `/* Computing loss` l `of sequence` $S = [s_0, s_1, s_2 \ldots s_{m+1}]$ `*/`
    for i *from* 1 *to* $m+1$ **do** `//` s_{m+1} `for EOS tokens`
      $\mathbf{h}_i \leftarrow LSTM_{\theta_T}^{hidden}(\mathbf{h}_{i-1}, f_{\theta_T}^{emb}(s_{i-1}))$
      $\widetilde{s}_i \leftarrow (f_{\theta_T}^{tu}(\mathbf{h}_i), f_{\theta_T}^{tv}(\mathbf{h}_i), f_{\theta_T}^{Lu}(\mathbf{h}_i), f_{\theta_T}^{Luv}(\mathbf{h}_i), f_{\theta_T}^{Lv}(\mathbf{h}_i))$
      $l \leftarrow l + \sum_c (s_i[c] \log \widetilde{s}_i[c] + (1 - s_i[c]) \log (1 - \widetilde{s}_i[c]))$
    if $l < \lambda$ **then**
      $\mathcal{L}_T = \mathcal{L}_T + l$
  $\theta_T \leftarrow \theta_T - \alpha \nabla_{\theta_T} \mathcal{L}_T$
  $\lambda = \lambda * \gamma$ `// Increase difficulty periodically`
until *stopping criteria* `// Typically when validation loss is minimized`

Algorithm 3: Pseudocode of graph generation for target dataset D_T

Input : Fine tuned parameters θ_T of deep generative model p_{θ_T}
Output : Graph G
$S \leftarrow ()$
$s_0 \leftarrow SOS$
$i \leftarrow 0$
$\mathbf{h}_0 \leftarrow \mathbf{0}$
repeat
  $i \leftarrow i + 1$
  $\mathbf{h}_i \leftarrow LSTM^{hidden}_{\theta_T}(\mathbf{h}_{i-1}, f^{emb}_{\theta_T}(s_{i-1}))$
  `// Sample` s_i `from multinomial distributions parameterized using` $\mathbf{h}_i$
  $s_i.t_u \sim Multinomial(f^{t_u}_{\theta_T}(\mathbf{h}_i))$
  $s_i.t_v \sim Multinomial(f^{t_v}_{\theta_T}(\mathbf{h}_i))$
  $s_i.L_u \sim Multinomial(f^{L_u}_{\theta_T}(\mathbf{h}_i))$
  $s_i.L_{uv} \sim Multinomial(f^{L_{uv}}_{\theta_T}(\mathbf{h}_i))$
  $s_i.L_v \sim Multinomial(f^{L_v}_{\theta_T}(\mathbf{h}_i))$
  $S.append(s_i)$
until $EOS \in \{s_i.t_u, s_i.t_v, s_i.L_u, s_i.L_{uv}, s_i.L_v\}$ `// Check if any item of tuple` s_i `contains` EOS `symbol`
$G \leftarrow \mathcal{F}^{-1}(S)$ `// Convert DFScode back to graph`
return G

C Dataset Semantics

Biological Domain: Proteins are biomolecules consisting of long chain of amino acids. They are highly essential to our lives and significantly interesting in certain biomedical tasks such as *de novo* protein design[32, 33]. Enzymes, a set of specialized proteins, are catalysts that can speed up metabolic activities. In our work, we utilize the Enzyme dataset from the BRENDA enzyme database [34], which consists of protein tertiary structures. We convert enzymes to graphs where nodes represent secondary structures labeled into one of the three categories namely *helices*, *turns*, or *sheets*. This dataset does not have edge labels. The dataset is divided into six classes and each enzyme belongs to one of these classes, namely EC1, EC2, EC3, EC4, EC5, EC6. For our limited data learning setup, we consider learning to generate graphs belonging to a certain enzyme class as a task. We treat the datasets EC1, EC2, EC4, EC5, EC6 as auxiliary and EC3 as our target dataset, which consists of 100 enzymes.

Chemical Domain: Chemical compounds are composed of two or more atoms connected using chemical bonds. We utilize the following chemical compounds datasets to train and evaluate GSHOT.

AIDS-CA [23]: This dataset comprises of a set of molecules that displayed activity against HIV.

Breast, Lung, Yeast: Each of these three datasets contain molecules that were screened for activity against Breast cancer, Lung cancer and cancer in Yeast respectively [12].

Leukemia-Active: This dataset consists of compounds that are active against Leukemia [12].

In all chemical datasets, we convert compounds to labeled graphs where nodes represent atoms and their labels represent atom-type which are elements belonging to the chemical periodic table. Edges in the graphs represent bonds and edge labels encode the bond type i.e single, double, triple.

For the limited data learning setup for chemical domain, *Yeast*, *Breast*, and *Lung* are used as auxiliary datasets during meta-training. Further, we choose AIDS-CA and Leukemia-Active datasets as our target datasets. The reasons for this choice is **(1)** due to their relatively low availability of number of graph samples and **(2)** since they consist of compounds that are active against certain diseases, therefore have more practical utility.

Physics Domain: Physics-based simulations are commonly used to understand interactions among different objects[17–19]. Dynamical systems such as N-body springs can be converted into graph structures where nodes represent particles and edges represent connections between particles. We utilize the dataset of the N-body spring simulations [19]. It consists of N particles in a two-dimensional space partitioned into a 5×5 grid . Two particles are connected to each other via spring with a probability of 0.5. The label of a node is the partition it lies in. This system does not have edge labels[19]. For learning under limited data, we meta-train GSHOT on auxiliary datasets consisting of four and six particle systems and then fine-tune on graphs containing five particles.

Table 3: Summary of the datasets

#	Name	Domain	No. of graphs	$\lvert V\rvert$	$\lvert E\rvert$	$\lvert\mathbb{V}\rvert$	$\lvert\mathbb{E}\rvert$
1	Enzymes[11]	Biological	600	[2, 125]	[2, 149]	3	X
2	NCI-H23 (Lung)[12]	Chemical	24k	[6, 50]	[6, 57]	11	3
5	Yeast[12]	Chemical	47k	[5, 50]	[5, 57]	11	3
7	MCF-7 (Breast)[12]	Chemical	23k	[6, 111]	[6, 116]	11	3
6	Leukemia-Active[12]	Chemical	1900	[12, 107]	[12, 111]	11	3
6	AIDS-CA[12]	Chemical	328	[10, 189]	[10, 196]	11	3
8	N-body Spring[19]	Physics	1500	N	[3, 13]	25	X

D Experimental Setup and Reproducibility

All experiments are performed on a machine with Intel Xeon Gold 6284 processor with 96 physical cores, 1 NVIDIA A100 GPU card with 40GB GPU memory, and 512 GB RAM running Ubuntu 20.04 operating system.

D.1 Parameter details

We set hidden dimension of $f_\theta^{L_u}$, $f_\theta^{L_v}$, $f_\theta^{L_{uv}}$, $f_\theta^{t_u}$, $f_\theta^{t_v}$ to 512. We utilize *Adam optimizer* with learning rate as 0.003. Further to avoid over-fitting we use dropout with value of 0.2 and an L2 regularizer with value of 10^{-5}. We set batch size to 32. For meta-training of GSHOT we used K=15 and $\epsilon = 0.8$. For Enzyme we set $K = 50$ and $\epsilon = 0.5$. During fine-tuning, we used the value of the growth-factor γ=1.001 for both Leukemia-Active and Enzyme, 1.006 for AIDS-CA and 1.1 for 5-body spring. For all methods, we stop training when validation loss is minimized or there is less than 0.05% change in validation loss over a number of extended epochs.

D.2 Number of graphs generated

Since our test datasets are of different sizes, AIDS-CA (108), Leukemia-Active (900), Enzyme-EC3 (20), 5-body Spring (500), we generate a different number of graphs for each target dataset. Specifically, for Leukemia-Active we generate 2560 graphs, 1024 graphs each for AIDS-CA and 5-body spring, and for Enzyme EC3 we generate 512 graphs.

E Impact of Self-paced fine tuning

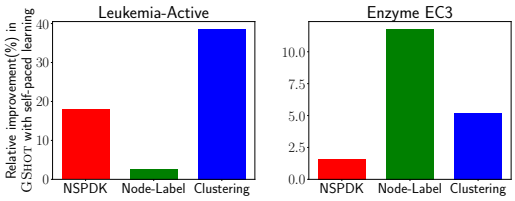

Figure 5: Ablation study showing the relative (%) improvement obtained by GSHOT when using *self-paced fine-tuning* compared to GSHOT with *vanilla fine-tuning*.

We study the improvement obtained by using *self-paced fine-tuning* in GSHOT over *vanilla fine-tuning* on different metrics. For a metric P, we define the improvement as $\frac{P_{\text{GSHOT}(vanilla)} - P_{\text{GSHOT}}}{P_{\text{GSHOT}}} \times 100$. Here, P_{GSHOT} refers to the value of the metric P obtained by our default model (with self-paced fine tuning), and $P_{\text{GSHOT}(vanilla)}$ refers to the value obtained by GSHOT with vanilla fine-tuning. In Fig. 5 we observe that a self-paced fine-tuning strategy can improve the fidelity metrics significantly.

F Impact of auxiliary datasets

In this section, we study the performance of our proposed architecture by selecting different auxiliary datasets during meta-training. Towards this, we choose Enzyme dataset since it consists of 5 auxiliary datasets and has reasonable scope to sample *multiple sets of auxiliary datasets* from it. For this experiment we sample(without repetition) sets of 3 auxiliary datasets 5 times(eg:- {EC1, EC4, EC5}, {EC2, EC5, EC6} etc.). We train 5 GSHOT models with these 5 different sets of auxiliary datasets. We then fine-tune these 5 trained models on the target dataset(EC3). We use the same set of auxiliary datasets for training the PRETRAIN+FT baseline. In Table 4, we report the mean performance on

each metric along with standard deviation obtained using these 5 models. For results of training graphGen and GRAPHRNN from scratch directly on the target dataset EC3(without auxiliary datasets), refer to Table 1 in the main paper.

Table 4: Performance on variation of auxiliary datasets: Performance comparison on the Enzyme EC3 dataset when different sets of auxiliary datasets are used for meta-training GSHOT and for training the PRETRAIN+FT baseline. For GSHOT and PRETRAIN+FT, we report the mean and standard deviation since their performance is averaged across models using different sets of auxiliary datasets used for (meta/pre) training.

Target dataset	Model	Deg.	Clus.	Orbit	NSPDK	Avg # Nodes (Gen/Gold)	Avg # Edges (Gen/Gold)	Node Label	Edge Label	Joint Node Label & Degree	Novelty	Uniqueness
Enzyme:EC3 #Training samples=50	PRETRAIN+FT	0.731 ±0.077	0.585 ±0.066	0.060 ±0.012	0.191 ±0.007	20.596/26.90 ±1.150	28.658/52.85 ±1.265	0.006 ±0.002	x x	0.644 ±0.026	98.50% ±0.005	98.70% ±0.004
	GSHOT	0.710 ±0.07	0.554 ±0.067	0.053 ±0.009	0.188 ± 0.005	20.742/26.90 ± 1.04	29.212/52.85 ± 1.27	0.004 ± 0.001	x x	0.634 ±0.018	98.11% ± 0.008	98.12% ± 0.009

In Table 4, we observe that GSHOT obtains superior performance when trained using different sets of auxiliary datasets. For instance, on the *Node label* metric, GSHOT outperforms its closest competitor PRETRAIN+FT by around 50%. Further, it outperforms its closest competitor by over 10% on the *Orbit* metric. Overall, we observe that GSHOT learns to better utilize the knowledge gained from a variety of auxiliary datasets.

G Learning to conditionally predict elements of edge tuple of DFS code

We assumed independence between components of edge tuple in order to simplify the modeling process. We also performed experiments by removing the independence assumption and making the prediction of components of edge tuple $\langle t_u, t_v, L_u, L_{uv}, L_v \rangle$ conditional on other elements. In order to model the conditional distribution, an order has to be imposed on the components of an edge tuple $\langle t_u, t_v, L_u, L_{uv}, L_v \rangle$. As discussed in Sec. 3.2, in the generation process of DFS code for a graph, first a node is discovered and consequently its discovery time t_u is recorded. Since this component depends upon the hidden state of the DFS code sequence, we first predict the timestamp t_u of the edge tuple using the hidden state h_i of LSTM. Now, in order to form an edge, the node with timestamp t_u is to be connected to node with discovery timestamp t_v. Since t_v depends upon the hidden state h_i and the timestamp t_u of the discovered node, we concatenate the hidden state embedding h_i and embedding $emb(t_u)$ of the timestamp t_u and predict the timestamp t_v. Now, for the remaining three components L_u , L_v and L_{uv}, we first predict the label of u and then v in order. This choice promises to improve likelihood of generating node labels L_v that have high probability of forming edges with nodes having label L_u and vice-versa. Finally, since the edge label between two nodes is a function of the node type(labels), therefore, we condition the edge label L_{uv} on the embedding of labels L_u and L_v of the edge tuple. The details of the conditional modeling are presented below:

$$
\begin{aligned}
t_u &= MLP(\mathbf{h}_i) \\
t_v &= MLP(\mathbf{h}_i | emb(t_u)) \\
L_u &= MLP(\mathbf{h}_i | emb(t_u) | emb(t_v)) \\
L_v &= MLP(\mathbf{h}_i | emb(t_u) | emb(t_v) | emb(L_u)) \\
L_{uv} &= MLP(\mathbf{h}_i | emb(t_u) | emb(t_v) | emb(L_u) | emb(L_v))
\end{aligned}
$$

Here emb refers to learnable embedding layer whose parameters are learnt during the training process.

To evaluate the performance of the above conditional prediction of the edge tuple, we ran experiments on the target dataset Leukemia-Active, Enzyme EC3 and AIDS-CA dataset . The results are presented in table 5. We denote the model with Independence assumption(default) as Ind, and the model with conditional prediction of components in edge tuple as Cond. On all datasets we observe that for the metrics Avg #nodes and Avg #edges, the models with conditional modeling of edge tuple convincingly outperforms the model(s) with the independence assumption. This signifies that sequence length has been better modelled in GSHOT when components of the edge tuple are modeled conditionally in comparison to when modeled independently. However, on the other distance metrics, we do not observe clear performance improvements.

Target dataset	Model	Deg.	Clus.	Orbit	NSPDK	Avg # Nodes (Gen/Gold)	Avg # Edges (Gen/Gold)	Node Label	Edge Label	Joint Node Label & Degree	Novelty	Uniqueness
Leukemia-Active	GSHOT (Ind)	0.0069	≈ 0	≈ 0	0.032	42.35/47.71	44.33/50.37	0.0011	≈ 0	0.24	100%	100%
	GSHOT (Cond)	0.01	≈ 0.003	≈ 0	0.06	46.37/47.71	49.23/50.37	0.003	≈ 0	0.44	100%	100%
AIDS-CA	GSHOT (Ind)	0.017	0.0015	≈ 0	0.08	26.5/37.14	27.1/39.60	0.011	≈ 0	0.14	99%	99%
	GSHOT (Cond)	0.01	0.004	≈ 0	0.07	28.44/37.14	30.50/39.60	0.007	≈ 0	0.12	98.33%	98.43%
Enzyme EC3	GSHOT (Ind)	0.45	0.47	0.025	0.16	24.5/26.90	37.69/52.85	0.004	x	0.457	100%	100%
	GSHOT (Cond)	0.43	0.60	0.03	0.20	27.50/26.90	42.55/52.85	0.007	x	0.58	99.4%	98.8%

Table 5: Conditional vs Independent modeling of edge tuple: Performance obtained by different models on different datasets on multiple metrics when components of edge tuples are predicted independently(Ind) vs when they are predicted conditionally(Cond).

H Using transformer for sequence Modelling

We integrated transformer [35] for modeling the sequences. We present the results in the table 6 when compared with current LSTM-based architecture.

On all datasets, we do not observe clear performance improvements.

Target dataset	Model	Deg.	Clus.	Orbit	NSPDK	Avg # Nodes (Gen/Gold)	Avg # Edges (Gen/Gold)	Node Label	Edge Label	Joint Node Label & Degree	Novelty	Uniqueness
Leukemia- Active	GSHOT (LSTM)	0.0069	≈ 0	≈ 0	0.032	42.35/47.71	44.33/50.37	0.0011	≈ 0	0.24	100	100
	GSHOT(Transformer)	0.0256	≈ 0.0067	≈ 0.0018	0.1983	50.22/47.71	54.57/50.37	0.011	≈ 0.00104	0.522	100	99.85
AIDS-CA	GSHOT (LSTM)	0.017	0.0015	≈ 0	0.08	26.5/37.14	27.1/39.60	0.011	≈ 0	0.14	99%	99%
	GSHOT (Transformer)	0.03044	0.001543	0.000680	0.100	27.10/37.14	28.64/39.60	0.02865	0.00089	0.2220	100%	99.70%
Enzyme EC3	GSHOT (LSTM)	0.45	0.47	0.025	0.16	24.5/26.90	37.69/52.85	0.004	x	0.457	100%	100%
	GSHOT (Transformer)	0.7827	0.5871	0.06490	0.2677	25.58/26.90	35.99/ 52.85	0.0177	x	0.6508	96.28%	97.38%

Table 6: Comparison of Transformer based model with LSTM(default) based modeling.

I Similarity of Target Dataset with Auxiliary Datasets and Impact on Performance

We compare our target datasets specifically Enzyme EC3 and Leukemia-Active with a variety of auxiliary datasets on different graph distance metrics in Table 7 below. For instance, we observe that Leukemia-Active target dataset has more similarities with chemical datasets such as Breast, Lung and Yeast. Additionally, we observe it is highly dis-similar with datasets belonging to Enzyme(Biological) category. Similarly, in Table 7 below we observe that Enzyme EC3 dataset is highly similar to other Enzyme datasets and dis-similar to datasets such as Breast, Lung and Yeast.

Further, to understand the impact of choosing different auxiliary datasets based upon their similarity to target dataset, we train GSHOT with different sets of auxiliary datasets. In Table 8, we observe GSHOT convincingly performs better when auxiliary datasets that are similar to target datasets are chosen for meta-training. Specifically, GSHOT trained with Yeast,Breast and Lung as auxiliary datasets significantly outperforms GSHOT meta-trained with Enzyme datasets, when the target dataset is Leukemia-Active. Similar conclusion is observed on Enzyme EC3 dataset in Table 8.

Target dataset	Auxiliary Dataset	Deg.	Clus.	Orbit	NSPDK	Avg # Nodes (Target/Aux)	Avg # Edges (Target/Aux)	Node Label	Edge Label	Joint Node Label & Degree
Leukemia-Active	**Breast**	0.007	0.0008	0.0003	0.07	47.0/55.83	49.61/59.35	0.007	≈ 0	0.029
	Lung	0.001	≈ 0	0.0002	0.065	47.0/40.0	49.61/41.82	0.012	≈ 0	0.05
	Yeast	0.0044	≈ 0	≈ 0	0.07	47.0/32.70	49.61/34.03	0.02	0.002	0.059
	Enzyme EC1	1.41	1.28	0.16	0.47	47.0/29.73	49.61/58.52	1.85	x	1.15
	Enzyme EC2	1.33	1.22	0.15	0.49	47.0/32.88	49.61/63.16	1.91	x	1.36
	Enzyme EC3	1.36	1.28	0.25	0.47	47.0/28.91	49.61/56.50	1.87	x	1.16
	Enzyme EC4	1.39	1.18	0.22	0.48	47.0/37.47	49.61/74.00	1.90	x	1.25
	Enzyme EC5	1.23	1.12	0.10	0.46	47.0/27.61	49.61/51.17	1.89	x	1.09
	Enzyme EC6	1.28	1.31	0.09	0.48	47.0/30.49	49.61/60.01	1.90	x	1.34
Enzyme EC3	**Enzyme EC1**	0.042	0.20	0.03	0.055	28.35/39.85	53.89/70.63	0.007	x	0.08
	Enzyme EC2	0.024	0.09	0.04	0.055	28.35/28.44	53.89/70.63	0.029	x	0.12
	Enzyme EC4	0.021	0.11	0.008	0.050	28.35/37.79	53.89/74.27	0.012	x	0.047
	Enzyme EC5	0.007	0.088	0.008	0.056	28.35/33.6	53.89/64.33	0.024	x	0.05
	Enzyme EC6	0.031	0.42	0.05	0.054	28.35/30.33	53.89/59.99	0.019	x	0.096
	Yeast	1.39	1.28	0.27	0.47	28.35/34.63	53.89/56.09	1.86	x	1.11
	Breast	1.37	1.287	0.26	0.49	28.35/44.01	53.89/46.26	1.89	x	1.15
	Lung	1.39	1.288	0.271	0.46	28.35/36.63	53.89/38.40	1.875	x	1.121

Table 7: Distance of target datasets with different auxiliary datasets on a variety of distance metrics. The auxiliary datasets highlighted in bold are highly similar to the target datasets.

Target dataset	Auxiliary Dataset	Model	Deg.	Clus.	Orbit	NSPDK	Avg # Nodes (Gen/Gold)	Avg # Edges (Gen/Gold)	Node Label	Edge Label	Joint Node Label & Degree	Novelty	Uniqueness
Leukemia-Active	Yeast, Breast, Lung	GSHOT	0.0069	≈ 0	≈ 0	0.032	42.35/47.71	44.33/50.37	0.0011	≈ 0	0.24	100%	100%
	Enzyme(1,2,3,4,5,6)	GSHOT	0.07	0.005	0.001	0.20	39.38/47.71	41.32/50.37	0.022	≈ 0	1.08	100%	100%
Enzyme EC3	Enzyme(1,2,4,5,6)	GSHOT	0.45	0.47	0.025	0.16	24.5/26.90	37.69/52.85	0.004	x	0.457	100%	100%
	Yeast, Lung, Breast	GSHOT	0.54	0.62	0.029	0.21	22.89/26.90	34.33/52.85	0.007	≈ 0	0.62	99.8%	99.8%

Table 8: Impact of different auxiliary datasets on quality of GSHOT. We observe that when auxiliary datasets are similar to target dataset(as per table 7), the performance of GSHOT is significantly better.